

## Dielectric properties of silver-gelatin granular suspensions

V. A. Davis\* and L. Schwartz

*Schlumberger-Doll Research, Old Quarry Road, Ridgefield, Connecticut 06877-4108  
and Physics Department, Brandeis University, Waltham, Massachusetts 02254-9110*

(Received 26 August 1985; revised manuscript received 16 December 1985)

Recently, some authors have employed a lattice-gas version of the coherent-potential approximation (LG-CPA) to describe the optical properties of composites formed by the suspension of Ag grains in a gelatin host. We show here that a direct approach to structural disorder, based on Roth's effective-medium approximation (EMA), yields results that are, at least, of comparable accuracy to those of the LG-CPA. The dependence of the EMA dielectric function on the input parameters that characterize metal-insulator suspensions is examined and found to be physically reasonable.

### I. INTRODUCTION

Suspensions form an important class of disordered composite materials.<sup>1-5</sup> In these systems, one of the two constituents exists in the form of isolated inclusions in a matrix of the host component. The dielectric properties of suspensions are of interest for a variety of reasons. One is that composites made of metallic particles embedded in an insulating matrix are especially efficient absorbers of solar radiation.<sup>6</sup> The present paper is concerned with metal-insulator suspensions. We confine ourselves to a particularly simple class of materials, those in which the (metallic) inclusions are spheres of a fixed radius. The interesting features of this problem are related to the strong scattering properties of the individual grains and the fact that the grain density need not be small.

The simplest theoretical approach to the calculation of the dielectric properties of suspensions is the average- $t$ -matrix approximation (ATA).<sup>1-4</sup> (The ATA is often referred to as the Maxwell Garnett approximation.<sup>3</sup>) The utility of the ATA is limited by the fact that it includes only the effects of dipole scattering by the inclusions and does not contain any information (beyond the average packing fraction) about their spatial distribution. Thus, it is not surprising that the ATA does not describe properly either the position or the width of the measured absorption peak in metal-insulator suspensions. Liesch and co-workers<sup>4</sup> have recognized the need to improve upon the ATA and have considered in some detail a Ag-gelatin composite studied experimentally by Kreibig.<sup>5</sup> Rather than dealing directly with topological disorder, these authors have proposed a lattice-gas (LG) model in which *structural* disorder is replaced by *substitutional* disorder. The suspension is modeled as a partially occupied lattice of spheres (i.e., an alloy of inclusions and vacancies) and its dielectric properties are calculated using an alloy version of the coherent-potential approximation (CPA). The results of their LG-CPA calculations are in significantly better agreement with measured data than corresponding ATA calculations.<sup>4</sup>

In an earlier paper<sup>1</sup> we have applied Roth's effective-medium approximation<sup>7</sup> (EMA) to the dielectric response of structurally disordered suspensions. The EMA pro-

vides a more complete description of correlations in the arrangement of the inclusions and, therefore, a more accurate description of the plasmon resonance in metal-insulator composites. While the EMA and LG-CPA represent quite different approaches, it is of interest to compare directly the results of calculations based on the two methods. Such a comparison is made in Sec. II of this paper. Interestingly, we find that, at least for the Ag-gelatin suspension considered by Kreibig, the results of these two approximation schemes are essentially identical. It is satisfying to see that qualitatively reasonable results can be obtained using a framework that attempts to deal directly with *structural* disorder (i.e., without invoking an *ad hoc* crystal lattice).

In setting up an EMA calculation,<sup>1</sup> four independent parameters must be specified. These are (1)  $j_{\max}$ , the highest-order scattering multipole, (2)  $\eta$ , the inclusion packing fraction, (3)  $a$ , the radius of an individual inclusion, and (4)  $g(R)$ , the pair distribution function. In Sec. III, the dependence of the EMA on these parameters is explored for a slightly simplified model of Ag-gelatin composites. The position and shape of the EMA absorption peak depend on these parameters in a way which is consistent with the physical picture of a system of interacting resonant levels.

### II. COMPARISON BETWEEN THEORY AND EXPERIMENT

Kreibig<sup>5</sup> has measured the dielectric response of a suspension of silver spheres (radius  $a=50$  Å) in gelatin ( $\epsilon_0=2.37$ ). His data show a well-defined plasmon resonance peak in the absorption spectra. The structure of this peak provides the basis for our comparison of alternate theoretical approaches. To describe the Ag inclusions we use an experimental silver dielectric function,<sup>8</sup> which has been modified,<sup>4</sup> to take into account the reduced electron mean free path due to defects observed in the silver. For spheres this small, the resonance is at  $ka \equiv 2\pi a/\lambda \sim 0.1$ , which is well within the long-wavelength regime. In Fig. 1(a) the measured absorption ( $\beta(\omega) = (\omega/c)\text{Im}[\sqrt{\epsilon(\omega)}]$ ) is compared with the results of

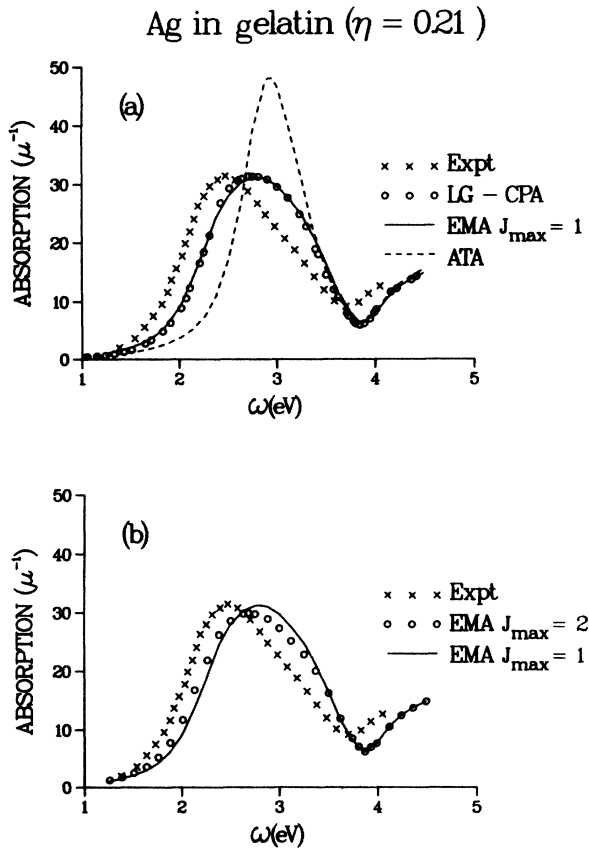


FIG. 1. In (a) the ATA, LG-CPA, and EMA ( $j_{\max}=1$ ) absorptions ( $\beta(\omega)=(\omega/c)\text{Im}[\sqrt{\epsilon(\omega)}]$ ) are compared with experimental results (Ref. 5) for 50-Å-radius Ag spheres. In (b) the EMA ( $j_{\max}=1$ ) and EMA ( $j_{\max}=2$ ) absorptions are compared with the same experimental data.

ATA, LG-CPA, and (dipole) EMA calculations. As expected,<sup>1,4</sup> the ATA peak is too narrow and is centered at a noticeably higher frequency than the experimental peak. The LG-CPA and EMA results are clearly in better agreement with experiment. In Figs. 1(b), we consider the influence of quadrupole terms on the EMA absorption peak. (We emphasize that the EMA is one of very few approaches which include higher-order multipole effects at long wavelengths.<sup>9</sup>) While such effects are not expected to be very important for  $\eta=0.21$ , the  $j_{\max}=2$  curve in Fig. 1(b) shows that they are noticeable, and that they shift the absorption curve toward somewhat better agreement with experiment.

### III. METAL SPHERES IN GELATIN

We turn now to a more general exploration of the EMA predictions for metal-insulator suspensions. To be specific, we again study Ag inclusions in a gelatin host ( $\epsilon_0=2.37$ ). For simplicity, we use a Drude representation [ $\epsilon_s(\omega)=\epsilon_b-\omega_p^2/(\omega^2+i\omega/\tau)$ ] for the Ag spheres. The Drude parameters are  $\epsilon_b=5.95$ ,  $\omega_p=9.2$  eV, and  $1/\tau=0.1$

eV.<sup>4</sup> This value of  $1/\tau$  corresponds to a free-electron path of about 100 Å. Most of the calculations were done for systems in which the sphere radius  $a=100$  Å. At wavelengths corresponding to 4.0 eV, the value of  $ka\sim 0.2$  and we are again within the long-wavelength limit over the frequency range of interest.

The first issue we examine is the effect of higher-order multipole interactions. We have already seen in Fig. 1(b) that, for a system with  $\eta=0.21$ , the inclusion of quadrupole terms produces a slight shift in the position of the absorption peak. To better illustrate this effect, Fig. 2 compares dipole and dipole-plus-quadrupole EMA results for  $\eta=0.10, 0.21$ , and  $0.30$ . On physical grounds, one expects that the influence of the quadrupole terms should become more significant for larger  $\eta$ . This effect is clearly evident in Fig. 2. (For  $\eta=0.30$ , the quadrupole effect is sufficiently strong that we might expect an additional contribution from the octopole terms.) To summarize the behavior of the EMA as a function of packing fraction, Fig. 3 shows the position of the absorption peak as a function of the packing fraction for the ATA and the EMA ( $j_{\max}=2$ ). This graph highlights the fact that the shift in the resonance position is enhanced with increasing packing fraction.

The next issue we consider is the sphere size and the role it plays in the calculation. The existence of the plasmon resonance and its position are due to effects unrelated to the size of the spheres (as long as they are small with respect to the wavelength). In Fig. 4, calculations with  $a=100$  and 200 Å are compared. (To avoid confusing two separate effects, the same Ag dielectric function was used in both calculations, even though the electron mean free path for the  $a=200$  Å spheres is somewhat longer than that for the  $a=100$  Å spheres.) Similarly, to

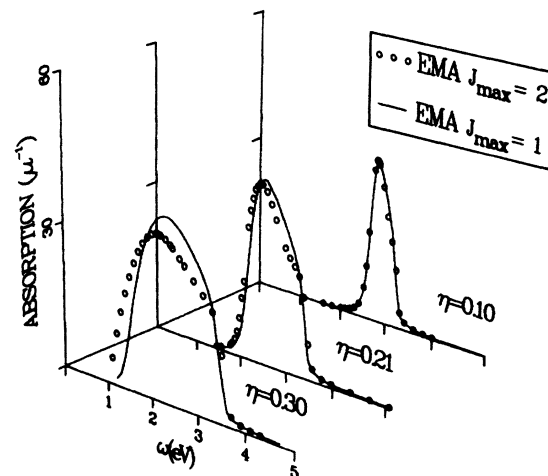


FIG. 2. EMA absorption for Ag spheres ( $a=100$  Å) embedded in gelatin with  $j_{\max}=1$  and  $j_{\max}=2$  are compared for three packing fractions. (Note that the peak positions for  $\eta=0.21$  are at slightly lower frequencies than the corresponding positions in Fig. 1; this is a consequence of the fact that different parameters were used to represent the dielectric function of the Ag spheres in the two calculations.)

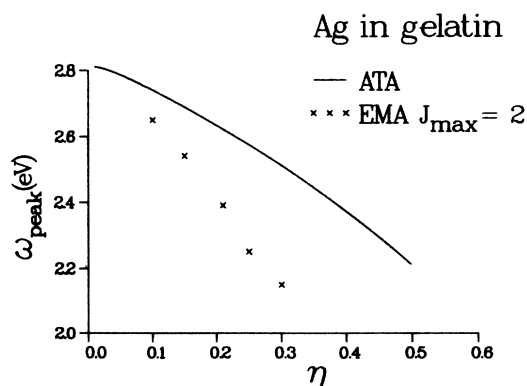


FIG. 3. Position of the absorption peak for Ag spheres ( $a=100 \text{ \AA}$ ) embedded in gelatin as a function of packing fraction for the ATA and the EMA with  $j_{\max}=2$ .

keep the packing fraction constant in the two calculations,  $g(R)$  was rescaled for the larger inclusions with the relation  $g(R) \rightarrow g(2R)$ . Note that the two sphere sizes lead to absorption peaks that are quite similar. This result is due to competition between two effects: (1) for isolated inclusions, larger sphere sizes correspond to broader dipole resonances, and (2) the distance between the sphere centers is greater (since  $\eta$  is held constant) for the larger inclusions. Since the two effects scale, respectively, as  $a^3$  and  $a^{-3}$ , the degree of compensation seen in Fig. 4 is not surprising. Also evident in this figure is a slight enhancement of the structure at the upper edge of the absorption peak for the suspension of 200- $\text{\AA}$  spheres. We believe that this is a consequence of the fact that the length scales characterizing the wavelength and the sphere diameter (or separation) are closer for the larger inclusions.

Finally, we consider the role of the pair distribution function in multiple-scattering calculations. The calculations presented in Figs. 1–4 are based on the pair distri-

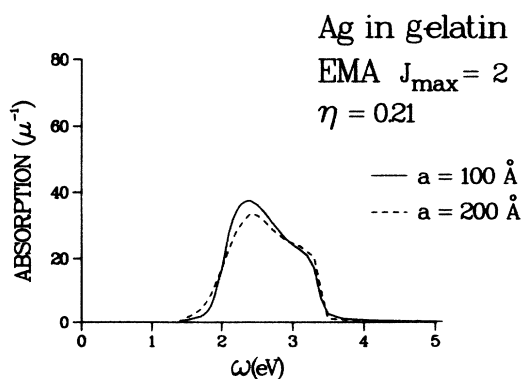


FIG. 4. EMA ( $j_{\max}=2$ ) absorption for Ag spheres embedded in gelatin with  $\eta=0.21$  for  $a=100 \text{ \AA}$  compared with the same for  $a=200 \text{ \AA}$ .

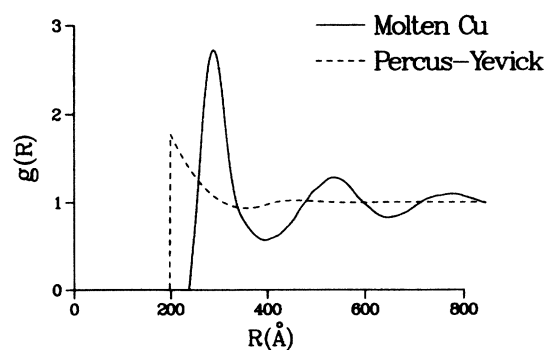


FIG. 5. Pair distribution functions used in this paper. The molten Cu and Percus-Yevick distributions are obtained, respectively, from experiment and calculation.<sup>11</sup>

bution function that describes the arrangement of Cu atoms in molten Cu at  $1150^\circ\text{C}$ .<sup>10,11</sup> Liquid Cu is a typical *close-packed* disordered system and the relevant diffraction data<sup>11</sup> indicate that its packing fraction is close to that of the suspensions of interest here (i.e.,  $\eta \approx 0.25$ ). This distribution function can easily be rescaled to treat systems with other packing fractions. In Fig. 5, the molten Cu distribution function is compared with a Percus-Yevick<sup>11</sup> hard-sphere distribution. We have found that the EMA shows a physically reasonable dependence on the choice of  $g(R)$ . In Fig. 6 we compare the EMA absorption curves (computed with  $j_{\max}=2$ ) for the two pair distributions shown in Fig. 5. The broadening of the resonance in the Percus-Yevick case is due to the fact that this distribution provides a wider range of nearest-neighbor distances and is analogous to corresponding effects noted in Ref. 10. Figure 6 illustrates that the pair distribution function plays a significant role in the calculation, but the overall trends of the solution are similar for different distributions.

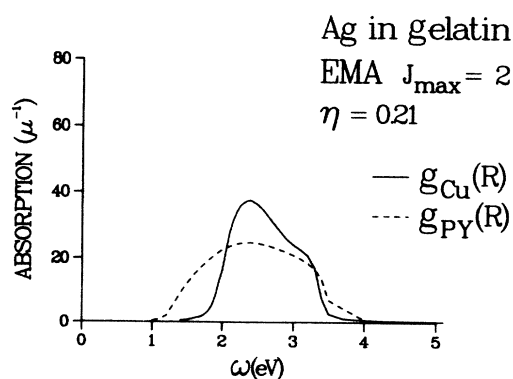


FIG. 6. EMA ( $j_{\max}=2$ ,  $a=100 \text{ \AA}$ ) absorption curves calculated using the molten Cu and Percus-Yevick distribution functions are compared.

- \*Present address: S-CUBED, Maxwell Laboratories, Inc., P.O. Box 1620, La Jolla, CA 92038-1620.
- <sup>1</sup>V. A. Davis and L. Schwartz, *Phys. Rev. B* **31**, 5155 (1985).
- <sup>2</sup>W. Lamb, D. M. Wood, and N. W. Ashcroft, *Phys. Rev. B* **21**, 2248 (1980).
- <sup>3</sup>J. C. Maxwell Garnett, *Philos. Trans. R. Soc. London* **203**, 385 (1904).
- <sup>4</sup>B. N. J. Persson and A. Liebsch, *Solid State Commun.* **44**, 1637 (1982); A. Liebsch and B. N. J. Persson, *J. Phys. C* **16**, 5375 (1983); Ansgar Liebsch and Pedro Villasenor Gonzalez, *Phys. Rev. B* **29**, 6907 (1984).
- <sup>5</sup>U. Kreibig, *Z. Phys. B* **31**, 39 (1978); U. Kreibig, A. Althoff, and H. Pressmann, *Surf. Sci.* **106**, 308 (1981).
- <sup>6</sup>A useful review is *Electrical Transport and Optical Properties of Inhomogeneous Media*, edited by J. C. Garland and D. B. Tanner (AIP, New York, 1978).
- <sup>7</sup>L. Roth, *Phys. Rev. B* **9**, 2476 (1974).
- <sup>8</sup>P. B. Johnson and R. W. Christy, *Phys. Rev. B* **6**, 4370 (1972).
- <sup>9</sup>The way that higher multipoles contribute to the long-wavelength behavior of the dielectric function is discussed in detail by Lamb Wood and Ashcroft.<sup>2</sup> These authors use a simple-cubic lattice with a large unit cell to treat disordered suspensions. While the width of their calculated absorption peak (cf. Fig. 4 of Ref. 2) is reasonable, they find a considerable amount of fine structure within the plasmon peak. This structure appears to be an artifact associated with the underlying lattice.
- <sup>10</sup>D. M. Nicholson, A. Chowdhary, and L. Schwartz, *Phys. Rev. B* **29**, 1633 (1984).
- <sup>11</sup>Y. Waseda, *The Structure of Non-Crystalline Materials* (McGraw-Hill, New York, 1980).